

Role of phonon scattering in carbon nanotube field-effect transistors

Jing Guo^{a)}

Department of Electrical and Computer Engineering, University of Florida, Gainesville, Florida 32611

Mark Lundstrom

School of Electrical and Computer Engineering, Purdue University, West Lafayette, Indiana 47907

(Received 21 October 2004; accepted 16 March 2005; published online 2 May 2005)

The role of phonon scattering in carbon nanotube field-effect transistors (CNTFETs) is explored by solving the Boltzmann transport equation using the Monte Carlo method. The results show that elastic scattering in a short-channel CNTFET has a small effect on the source-drain current due to the long elastic mean-free path (mfp) ($\sim 1 \mu\text{m}$). If elastic scattering with a short mfp were to exist in a CNTFET, the on current would be severely degraded due to the one-dimensional channel geometry. At high drain bias, optical phonon scattering, which has a much shorter mfp ($\sim 10 \text{ nm}$), is expected to dominate, even in a short-channel CNTFET. We find, however, that inelastic optical scattering has a small effect in CNTFETs under modest gate bias. © 2005 American Institute of Physics. [DOI: 10.1063/1.1923183]

Carbon nanotube field-effect transistors (CNTFETs) are now being explored for high-performance electronics.^{1,2} A recently reported CNTFET with a channel length of $\sim 50 \text{ nm}$ appears to deliver a near-ballistic current.³ This is a surprising result, because under high drain bias the channel is expected to be several mean-free-paths (mfps) long. Previous studies have shown that the dominant scattering mechanism in a high-quality carbon nanotube (CNT) is phonon scattering.⁴⁻⁷ Under low bias, the mfp is observed to be very long in CNTs ($\sim 1 \mu\text{m}$), and is thought to be nearly elastic and limited by acoustic phonon (AP) scattering.⁵ Under high bias, optical phonon (OP) emission dominates, and short ($\sim 10 \text{ nm}$) mfps result. In metallic CNTs, OP emission leads to a high-bias saturation current of $\sim 25 \mu\text{A}$ for a long tube and a significant decrease of channel conductance for a short tube.^{6,7} Studies of phonon scattering in CNTs have focused on metallic tubes or on long semiconducting tubes.⁸ Phonon scattering in short-channel CNTFETs, which is important for nanoelectronic applications, remains unexplored.

In this letter, we show that near-ballistic dc currents can be obtained for a short-channel CNTFET even under high source-drain bias in the presence of significant inelastic scattering. The results indicate that elastic scattering has a small effect on the source-drain current for a short-channel CNTFET when the elastic mfp is long. If, however, a short elastic mfp were to exist in a CNTFET, elastic scattering would degrade the on current of CNTFETs much more severely than it does for a typical metal-oxide-semiconductor field-effect transistor (MOSFET). This difference results from the difference between one-dimensional (1D) transport in a CNT and two-dimensional (2D) transport in a MOSFET channel, and generally applies to all nanotube/nanowire transistors with 1D channel geometry.⁹

To treat phonon scattering in CNTFETs, we simulate semiclassical transport by the Monte Carlo (MC) method self-consistently coupled to the Poisson equation. The validity of a semiclassical approach for treating a short-channel CNTFET ($L_{\text{ch}} \sim 20 \text{ nm}$) was first confirmed by a full quantum simulation under ballistic conditions.¹⁰ The MC simulation simulates stochastic carrier trajectories and has been ex-

tensively applied to study the dissipative carrier transport in Si MOSFETs.¹¹ It has also been applied to study carrier transport in CNTs,⁸ and calibrated to experiments for a metallic tube with length down to $\sim 50 \text{ nm}$.⁶ Two scattering mechanisms have been identified to be important in metallic CNTs,⁶ and were included in this study, acoustic phonon scattering and OP scattering (including phonons with both small wave vector $k \sim 0$ and large k near the Brillouin zone edge).⁷

We describe the first conduction subband E - k using a simple analytical expression derived from a p_z orbital tight-binding model,¹²

$$E = \hbar v_F (\sqrt{k^2 + k_0^2} - k_0), \quad (1a)$$

where E is the kinetic energy, \hbar is the Planck constant, $v_F \approx 8.0 \times 10^7 \text{ cm/s}$ is the Fermi velocity in a metallic tube, and $k_0 = 2/(3d)$, where d is the diameter of the tube. The corresponding density of states (DOS) is

$$D(E) = D_0 \cdot \frac{|E + \Delta|}{\sqrt{(E + \Delta)^2 - \Delta^2}} \Theta(E), \quad (1b)$$

where $D_0 = 4/(\pi \hbar v_F)$ is the constant DOS of a metallic tube, and Δ is one-half of the band gap, and $\Theta(x)$ equals 1 for $x > 0$ and 0 for $x \leq 0$. Only the lowest subband is treated; the effect of higher subbands will be discussed later.

In a metallic tube, the scattering rates and mfps are energy independent due to the constant DOS near the Fermi level, but in a semiconducting tube, the scattering rates and mfps are energy dependent. Note that the band structure of a

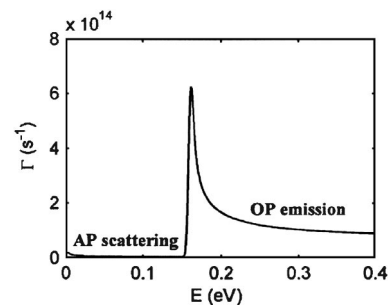


FIG. 1. Scattering rate vs carrier kinetic energy in the lowest subband.

^{a)}Electronic mail: guoj@ece.ufl.edu

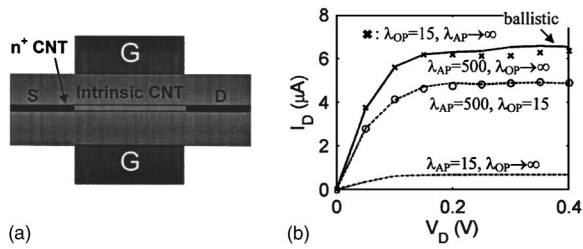


FIG. 2. Scattering in CNT MOSFETs: (a) A coxially gated CNTFET with doped source/drain. The tube diameter is $d \sim 1.4$ nm with a band gap $E_g \sim 0.6$ eV. The total tube length is 50 nm, with an intrinsic channel of $L_{ch} = 20$ nm, and a doped source/drain of $L_S = L_D = 15$ nm. The gate oxide thickness is $t_{ox} = 3$ nm, and the dielectric constant is $\kappa = 16$. (b) The simulated I_D vs V_D at $V_G = 0.4$ V for five cases: (i) solid: Ballistic transport, (ii) crosses: OP scattering only, with $\lambda_{OP}^{high} = 15$ nm and $\lambda_{elastic} \rightarrow \infty$, (iii) dashed: Elastic scattering only, with $\lambda_{elastic}^{high} = 500$ nm and $\lambda_{OP} \rightarrow \infty$, (iv) Circles: elastic and OP scattering with $\lambda_{elastic}^{high} = 500$ nm and $\lambda_{OP}^{high} = 15$ nm, and (v) dash-dot: Strong elastic scattering with $\lambda_{elastic}^{high} = 15$ nm and $\lambda_{OP} \rightarrow \infty$.

semiconducting tube at high energies approaches that of a metallic tube, so the mfps of a semiconducting tube at high energies, $\lambda_{elastic}^{high}$ and λ_{OP}^{high} also approach those of a metallic tube. The scattering rate in a semiconducting tube, as shown in Fig. 1, is computed by

$$\frac{1}{\tau(E)} = \frac{v_F}{\lambda_{elastic}^{high}} \frac{D(E)}{D_0} + \frac{v_F}{\lambda_{OP}^{high}} \frac{D(E - \hbar\omega_{OP})}{D_0}, \quad (2)$$

where $\lambda_{elastic}^{high} = 500$ nm is a typical high-energy mfp for AP scattering, $\lambda_{OP}^{high} = 15$ nm is a typical high-energy mfp for OP scattering, and $\hbar\omega_{OP} = 0.16$ eV is a typical OP energy.⁶ Only OP emission was treated because at thermal equilibrium, $\hbar\omega_{OP} \gg k_B T$, so the phonon population is small. (The effect of hot phonons will be discussed later.)

Pauli blocking is an important factor that is treated using a rejection technique as described by Lugli.¹³ The carrier distribution function is updated after each time step, so that when a scattering event occurs, the probability that the final state is available can be evaluated. A random number between 0 and 1 then determines whether the scattering is permitted. To treat transistor electrostatics, Poisson's equation is solved self-consistently with the transport simulation. Two types of contacts are treated. For a CNT MOSFET with doped tubes as source/drain shown in Fig. 2(a),¹⁴ the contacts are assumed to be ideal (without reflection). For CNT Schottky barrier (SB) FETs as shown in the inset of Fig. 4(a),¹⁵ we treat the tunneling of carriers through metal-CNT junctions as follows. For a carrier injected to a SB, the transmission probability through the SB is evaluated using the Wentzel-Kramers-Brillouin approximation. A random number between 0 and 1 is then generated to determine whether the carrier tunnels through the SB or gets reflected. Such an approach has been previously developed to treat Si SBFETs, and validated by experiments for a channel length of < 30 nm.¹⁶

We first simulated a CNT MOSFET with doped tubes as source/drain extensions, as shown in Fig. 2(a). To explore the role of elastic scattering in CNTFETs, we first treated only elastic scattering in the CNT channel and omitted OP scattering ($\lambda_{OP}^{high} \rightarrow +\infty$). For a long elastic mfp of $\lambda_{elastic}^{high} = 500$ nm [which is typical for a high-quality CNT (Ref. 6), and results in a thermal average mfp $\langle \lambda_{elastic} \rangle \sim 90$ nm near the top of the barrier], the transistor delivers $\sim 80\%$ of the ballistic on current, as shown by the dashed line in Fig. 2(b).

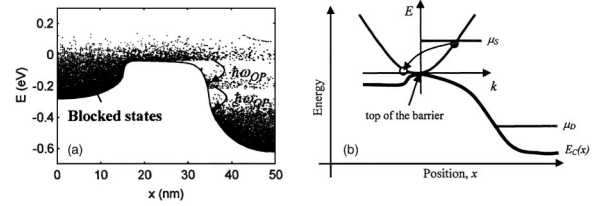


FIG. 3. Optical phonon scattering in CNTFETs: (a) A snapshot of the electron distribution at the steady state for $V_D = V_G = 0.4$ V with $\lambda_{OP}^{high} = 15$ nm and $\lambda_{elastic}^{high} = 500$ nm. The solid line shows the first subband edge. (b) A sketch for OP scattering at a large gate overdrive. $E-k$ at the top of the barrier, E_{top} is also shown. μ_S and μ_D are the source and drain Fermi levels, respectively.

Elastic scattering has a rather small effect because of the long elastic mfp. In contrast, for a short elastic mfp of $\lambda_{elastic}^{high} = 15$ nm (which corresponds to a thermal average mfp of $\langle \lambda_{elastic} \rangle \sim 3$ nm near the top of the barrier), the transistor only delivers $\sim 10\%$ of the ballistic current, as shown by the dashed-dotted line.

Compared to a Si MOSFET, elastic scattering has a much stronger effect for a CNTFET. It has been reported that Si MOSFETs with a channel length several times longer than the elastic scattering mfp (due to, for example, surface roughness scattering) can still operate at nearly 50% of the ballistic limit.^{17,18} This difference results from the difference between 1D carrier transport in a CNT channel and 2D in a MOSFET channel. For a MOSFET, the final k states for an elastic scattering event distribute in (k_x, k_y) plane. For most final states, a carrier does not possess enough backward velocity along the channel direction after an elastic scattering event to overcome the barrier, and return to the source. For this reason, scattering near the drain has much less of an effect on I_D than scattering near the source end of the channel.¹⁹ (Of course, scattering near the drain causes the space-charge density to build up, which has an indirect, though potentially strong, effect on the current of a short-channel MOSFET.)^{20,21} In contrast, for a carrier with a wave vector $+k$ in a CNT, the only available final state after a scattering event is $-k$, because of the one-dimensional channel geometry. The magnitude of carrier velocity along the channel direction remains unchanged and the carrier can overcome the top of the barrier and return back to the source. Elastic scattering anywhere in the channel affects the source-drain current equally. The effect of a short-mfp-elastic scattering in a nanotube/nanowire transistor is much more severe than in a typical MOSFET. Because the elastic mfps are so long, however, we do not expect elastic scattering to have a strong effect on short-channel CNTFETs.

We next explore the role of inelastic optical phonon scattering, which has a much shorter mfp, and scatters carriers even in a short CNT at high biases.^{6,7} The circles in Fig. 2(b) show the current-voltage (I_D - V_D) characteristics in the presence of both elastic scattering (with $\lambda_{elastic}^{high} = 500$ nm) and OP scattering (with $\lambda_{OP}^{high} = 15$ nm). Compared to the I_D - V_D only in the presence of elastic scattering (with $\lambda_{elastic}^{high} = 500$ nm and $\lambda_{OP}^{high} \rightarrow \infty$), as shown by the dashed line, a short mfp OP scattering has little effect on I_D . Figure 3(a), which plots a snapshot of the steady-state carrier distribution at on state, explains the reason. Before a carrier injected from the source reaches the top of the barrier, Pauli exclusion suppresses OP emission. As shown in Fig. 3(a), the $-k$ states below the top of the barrier at the source end of the tube are filled according to the source Fermi level, and are full. OP emission low-

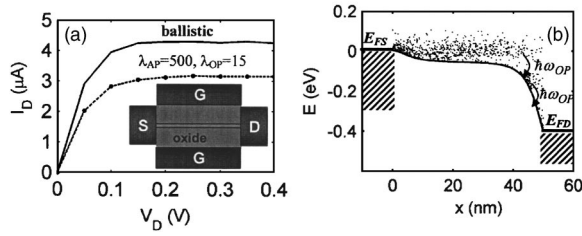


FIG. 4. Scattering in CNT SBFETs: (a) I_D vs V_D at $V_G=0.4$ V for ballistic transport (solid line), and in the presence of both elastic and OP scattering with $\lambda_{\text{elastic}}^{\text{high}}=500$ nm and $\lambda_{\text{OP}}^{\text{high}}=15$ nm (dashed line with circles). The inset shows the simulated CNTFET with metal source/drain. The SB height for electrons is $\phi_{Bm}=0$, the intrinsic channel length is 50 nm, and the tube diameter is $d\sim 1.4$ nm with $E_g\sim 0.6$ eV. The gate oxide thickness is 8 nm with a dielectric constant of $\kappa=16$. (b) A snapshot of the electron distribution at the steady state for $V_D=V_G=0.4$ V with OP and elastic scattering.

ers the carrier energy by $\hbar\omega_{\text{OP}}$, which results in a final state that is already occupied. Such a scattering event is prohibited by Pauli exclusion. After the carrier travels over the top of the barrier, OP emission can occur. Such OP emission, however, does not affect the dc source-drain current. At modest gate bias, the top of the barrier, E_{top} , is only modestly below the source Fermi level ($\mu_S - E_{\text{top}} < \hbar\omega_{\text{OP}}$). After OP emission, a carrier loses energy of $\hbar\omega_{\text{OP}}$ (~ 0.16 eV), and it does not have enough energy to overcome the barrier and return to the source. The large OP energy ($\hbar\omega_{\text{OP}}\sim 0.16$ eV) in CNTs helps the transistor to deliver a near-ballistic dc current at modest gate biases, although a significant amount of scattering exists near the drain end of the channel. We also simulated the I_D - V_D characteristics in the presence of only OP scattering with $\lambda_{\text{OP}}^{\text{high}}=15$ nm and $\lambda_{\text{AP}}^{\text{high}}\rightarrow\infty$, as shown by the crosses in Fig. 2(b). The transistor essentially delivers a ballistic source-drain current, which further confirms that the effect of short-mfp OP scattering is small.

We also explored the role of phonon scattering under high gate voltages, which pushes the top of the barrier, E_{top} , well below the source Fermi level, μ_S , as shown in Fig. 3(b). The results indicate that once $\mu_S - E_{\text{top}} > \hbar\omega_{\text{OP}}$, OP scattering begins to significantly affect the source-drain current. For a carrier injected with energy $E > E_{\text{top}} + \hbar\omega_{\text{OP}}$, after an OP emission event, the carrier is still energetic enough to overcome the top of the barrier and return back to the source. The result is that the current contributed by carriers with $E > E_{\text{top}} + \hbar\omega_{\text{OP}}$ is significantly reduced by OP scattering.

Because most CNTFETs, to date, operate like SB transistors,¹⁵ it is important to examine whether our understanding of CNT MOSFETs is relevant to CNT SBFETs. As shown in the inset of Fig. 4(a), the simulated CNTFET is similar to a recently reported CNTFET with Pd contacts,³ except that coaxial-gate geometry is used. The main panel of Fig. 4(a) plots the I_D versus V_D at the ballistic limit (the solid line), and with scattering (the dashed line). Again, we find that the CNT SBFET also delivers a near-ballistic source-drain current for the following reason. The elastic scattering has a small effect because of its long mfp. For OP scattering in the channel, a carrier loses energy of $\hbar\omega_{\text{OP}}$ after OP emission. Because of the large OP energy (~ 160 meV), the back-scattered carrier faces a much thicker and higher tunneling barrier, as shown in Fig. 4(b). Because the tunneling probability exponentially decreases with the SB thickness and height, the chance for the scattered carrier to return back to the source significantly decreases. OP scattering, therefore,

has little effect on the source-drain current at modest gate biases in a SB CNTFET.

As mentioned earlier, only the first subband is treated in this study, but an energetic carrier near the drain end of the channel can scatter to higher subbands. After a carrier is scattered to a higher subband, however, the potential barrier between the carrier and the source increases, and it becomes more difficult for the carrier to return back to the source. Intersubband scattering, therefore, will not change the conclusion that inelastic scattering has a small effect on the dc current. As also mentioned earlier, only OP emission was treated, because essentially no optical phonons are present at thermal equilibrium. Optical phonons, however, can build up and be reabsorbed by source-injected electrons. Detailed treatment of hot phonon effects requires solving electron-phonon-coupled Boltzmann transport equation, which is beyond the scope of this study. Simple estimation shows that most OPs are emitted when $+k$ going electrons are backscattered, and therefore, they possess a wave vector along $+k$ direction. When such OPs are reabsorbed, electrons are scattered toward the drain rather than back to the source, which does not lower the source-drain dc current. Our neglect of OP phonon emission and intersubband scattering is justified because this study is concerned with the effect of scattering on the dc current under high-bias conditions.

The authors thank A. Javey and Professor H. Dai of Stanford University for extensive discussions. This work was supported by the NSF Network for Computational Nanotechnology (NCN), the MARCO Focused Center on Materials, Structure, and Devices, and the start-up fund for one of the authors (J. G.) at the University of Florida.

- ¹M. Fuhrer, H. Park, and P. L. McEuen, IEEE Trans. Nanotechnol. **1**, 78 (2002).
- ²P. Avouris, J. Appenzeller, R. Martel, and S. Wind, Proc. IEEE **91**, 1772 (2002).
- ³A. Javey, J. Guo, D. B. Farmer, Q. Wang, D. Wang, R. G. Gordon, M. Lundstrom, and H. Dai, Nano Lett. **4**, 447 (2004).
- ⁴Z. Yao, C. L. Kane, and C. Dekker, Phys. Rev. Lett. **84**, 2941 (1999).
- ⁵D. Mann, A. Javey, J. Kong, Q. Wang, and H. Dai, Nano Lett. **3**, 1541 (2003).
- ⁶A. Javey, J. Guo, M. Paulsson, Q. Wang, D. Mann, M. Lundstrom, and H. Dai, Phys. Rev. Lett. **92**, 106804 (2004).
- ⁷J. Park, S. Rosenblatt, Y. Yaish, V. Sazonova, H. Ustunel, S. Braig, T. Arias, P. Brouwer, and P. McEuen, Nano Lett. **4**, 517 (2004).
- ⁸G. Pennington and N. Goldsman, Phys. Rev. B **68**, 045426 (2003).
- ⁹Y. Cui, Z. Zhong, D. Wang, W. Wang, and C. Lieber, Nano Lett. **3**, 149 (2003).
- ¹⁰J. Guo, S. Datta, M. Lundstrom, and M. P. Anantram, Int. J. Multiscale Comp. Eng. **2**, 257 (2004).
- ¹¹M. Fischetti and S. E. Laux, Phys. Rev. B **38**, 9721 (1988).
- ¹²J. W. Mintmire and C. T. White, Phys. Rev. Lett. **81**, 2506 (1998).
- ¹³P. Lugli and D. K. Ferry, IEEE Trans. Electron Devices **32**, 2431 (1985).
- ¹⁴J. Chen, C. Klinke, A. Afzali, and P. Avouris, Appl. Phys. Lett. **86**, 123108 (2004).
- ¹⁵S. Heinze, J. Tersoff, R. Martel, V. Derycke, J. Appenzeller, and P. Avouris, Phys. Rev. Lett. **89**, 106801 (2002).
- ¹⁶B. Winstead and U. Ravaioli, IEEE Trans. Electron Devices **47**, 1241 (2000).
- ¹⁷F. Assad, Z. Ren, D. Vasileska, S. Datta, and M. Lundstrom, IEEE Trans. Electron Devices **47**, 232 (2000).
- ¹⁸A. Lochtefeld and D. Antoniadis, IEEE Electron Device Lett. **22**, 95 (2001).
- ¹⁹M. Lundstrom and Z. Ren, IEEE Trans. Electron Devices **49**, 133 (2002).
- ²⁰A. Svizhenko and M. P. Anantram, IEEE Trans. Electron Devices **50**, 1459 (2003).
- ²¹R. Venugopal, M. Paulsson, S. Goasguen, S. Datta, and M. Lundstrom, J. Appl. Phys. **93**, 5613 (2003).